DOI: 10.53469/jpce.2025.07(11).07

Mountainous Areas Landslide Susceptibility Evaluation Based on Machine Learning

Shuhao Dong[1], Shengwu Qin[1,2]*, Jiangfeng Lv[1], Jiasheng Cao[1], Jingyu Yao[1], Jiayu Yan[1], Chaobiao Zhang[1]

[1]College of Construction Engineering, Jilin University, Changchun 130026, China
[2]Observation and Research Station of Geological Hazards and Geological Environment in Changbai Mountain Volcano, Ministry of Natural Resources, Changchun, China
Correspondence Author, qinsw@jlu.edu.cn

Abstract: ***Landslides pose a persistent threat in the geologically complex and ecologically fragile mountainous terrain of Yanbian Prefecture, Northeast China. To address this challenge, we propose an innovative susceptibility assessment framework that integrates ensemble machine learning with SHapley Additive exPlanations for interpretable prediction. Eleven critical environmental and anthropogenic factors—altitude, slope, aspect, curvature, lithology, land use, rainfall, TWI, NDVI, and distances to rivers and roads—were selected to build a comprehensive indicator system based on hydrological watershed units. A suite of advanced machine learning algorithms, including Random Forest, XGBoost, LightGBM, CatBoost, and AdaBoost, were employed and further optimized using ensemble strategies such as Stacking, Bagging, and Voting. Among them, the Stacking ensemble demonstrated superior predictive performance with the highest AUC value. More importantly, the integration of SHAP allowed for a transparent and quantitative interpretation of feature contributions, revealing that distance to roads, rainfall, and NDVI are the dominant drivers of landslide susceptibility in the region. This study not only advances the precision and interpretability of disaster prediction models but also offers practical insights for regional hazard mitigation, land-use planning, and sustainable ecological management.***

Keywords: Landslide susceptibility, Ensemble learning, Machine learning, Watershed unit.

1. Introduction

Landslide is a common geological hazard in mountainous areas, primarily triggered by factors such as precipitation, glacier meltwater, or earthquakes (He et al., 2022; Rickenmann et al., 2006). Its powerful impact and sedimentation capabilities often cause significant harm to production and daily life in the areas it flows through and accumulates (Iversion 1997; Jakob et al., 2013). For policymakers, mitigating landslide risks is challenging due to the uncertainty in predicting when and where they occur. Landslide susceptibility assessment is an important tool for identifying areas prone to landslides (Corominas et al., 2014; Cui et al., 2013; Shen et al., 2018). In recent years, thanks to significant scientific advances in physical/process-based models (Guzzetti 2003; Han et al., 2017) and statistical models (Anbalagan and Singh 1996; Liu 2003; Liu et al., 2020), the field has made significant breakthroughs, and several models and methods have been recommended for landslide susceptibility assessment. Physical/process-based models typically use random flow routing models (Scheild and Rickenmann 2011) or Navier-Stokes (N-S) equation based models (Pellegrino et al., 2015) to simulate the depth and velocity of landslides, thereby addressing the challenges of analyzing and predicting hazards. However, physical/process-based models depend on extensive field data, and for large-scale applications, the computational and economic costs required to obtain reliable results make their widespread use challenging.

In contrast, statistical models provide a more economical and less computationally demanding approach for predicting the spatial distribution of landslides (Di Napoli et al., 2020; Huang et al., 2021b). By assuming that factors responsible for past landslide occurrences will repeatedly trigger future events—i.e., the past is the key to the future—statistical models such as bivariate statistical analysis (Constantin et al., 2011), logistic regression (Tsangaratos and Ilia 2016), multiple regression (Felicísimo et al., 2013), and weights of evidence (Tsangaratos et al., 2017) have been widely regarded as suitable tools for assessing landslide susceptibility on a regional scale. In recent years, machine learning algorithms (Support Vector Machines (Pham et al., 2018), Artificial Neural Networks (Ermini et al., 2005), Decision Trees (Shaikhina et al., 2019), and Random Forests (Rigatti 2017) e.g.) have gained considerable attention within statistical methods. A growing number of researchers have obtained high-accuracy classifiers by employing these algorithms to capture the nonlinear relationships between landslide occurrences and their influencing factors. However, single models inherently involve certain uncertainties (Merghadi et al., 2018). Many scholars have therefore proposed minimizing these uncertainties by combining the predictive outputs of multiple algorithms (Chen et al., 2017a; Chen et al., 2017b; Dou et al., 2020). Ensemble learning algorithms have made substantial contributions to mitigating uncertainty and improving predictive accuracy. Inspired by the statistical regularities of random phenomena, these ensemble methods can yield superior predictions compared to individual classifiers (Zhang et al., 2022). Consequently, as highlighted by Dou et al (Dou et al., 2020), it is essential to explore new ensemble methods for landslide susceptibility mapping.

In addition, most susceptibility studies, both domestically and internationally, focus on optimizing machine learning models to achieve higher accuracy, with relatively little attention paid to the internal decision-making mechanisms of these models. Landslide formation is highly complex, and the regional characteristics of various influencing factors have a significant impact on landslide distribution (Hutter et al., 1994; Zeng et al., 2024). As highlighted in the review by Dikshit et al. (Dikshit et al., 2021), a lack of model interpretability is one

of the primary challenges currently faced when applying artificial intelligence in the geohazard domain. Previous research has often employed methods such as Pearson's correlation coefficient, the Gini index, and Geo Detector to interpret model outputs and the importance of influencing factors (Chen et al., 2018). For example, Lin et al. (Lin et al., 2021), examining a typical mountainous environment — Fujian Province—utilized an information-value model (which measures the information gain of geological hazard points under different factor classes) and the Geo Detector approach to systematically assess the regional distribution of geological hazards, as well as quantitatively analyze the key triggering factors and their interaction effects. While these methods offer insights at a global level, they lack the capacity to elucidate the specific factors driving predictions at the local or individual level. SHAP is an explainable AI technique that has recently attracted substantial attention (Marcílio and Eler 2020). The method offers a variety of visualizations that aid in clarifying the interdependencies among variables with respect to model outcomes (Zhang et al., 2023). This approach has been widely applied across multiple domains, including medical diagnostics and judicial decision-making assistance (Mokhtari et al., 2019; Wang et al., 2024). Pradhan et al (Pradhan et al., 2023). were the first to introduce SHAP into susceptibility research, illustrating and quantifying the importance and interactions of different influencing factors in a model. Their findings demonstrate that machine learning models combined with the SHAP method achieve superior decision-making performance and interpretability.

The primary contribution of this study lies in the application of ensemble learning algorithms and an interpretable model (SHAP) to landslide susceptibility modeling. The main objective is to quantitatively evaluate the influence of GIS-based ensemble models (Stacking, Boosting, and Voting) on landslide susceptibility in Yanbian Prefecture, China, and to validate and compare the performance of different models using performance metrics (the Area Under the Receiver Operating Characteristic Curve, AUC). Subsequently, SHAP is employed to elucidate the decision-making processes of these ensemble models, thereby promoting the effective use of such models in landslide hazard management and supporting planning and disaster reduction practices in the study region.

2. Study Area and Data Sources

2.1 Study Area

Yanbian Korean Autonomous Prefecture (hereafter referred to as Yanbian Prefecture) is located in eastern Jilin Province, China, spanning from 41°59′47″ N to 44°30′42″ N and 127°27′43″ E to 131°18′33″ E (Figure 1). There are several reasons for choosing Yanbian Prefecture as the study area. Firstly, Yanbian Prefecture represents a typical mountainous environment, with mountain areas occupying approximately 54.8% of the total area. The overall terrain exhibits considerable elevation differences and is characterized by three geomorphological gradients—mountains, hills, and basins—that facilitate landslide evolution. Secondly, the regional ecosystem plays a pivotal role within the ecological network of Northeast Asia, and its ecological conditions are closely tied to both the socioeconomic development and ecological security of Jilin Province. Finally, extensive preliminary investigations on landslide hazards have been conducted in Yanbian Prefecture, yielding a rich dataset of landslide occurrences and associated influencing factors, thus establishing a robust spatial data foundation for this study.

The study area encompasses approximately 4,330 km², with elevations ranging from 3 m to 2,659 m. The terrain is generally higher in the west and lower in the east, sloping from the southwest, northwest, and northeast toward the southeast. In addition, it falls under a temperate monsoon climate, with an annual mean temperature of 4.8°C and average yearly precipitation of about 640 mm—primarily concentrated between June and August. Precipitation is unevenly distributed, with the Changbai Mountain area receiving the highest rainfall in the region. As of late 2023 to early 2024, the permanent population is recorded at 1.8949 million. Granite constitutes the predominant lithology in this region, followed by basalt and shale. Situated in the heart of Northeast Asia, Yanbian Prefecture plays a key role in major economic development strategies, such as the Belt and Road Initiative (BRI), the Revitalization of Northeast China, and the 'Changchun–Jilin–Tumen' Pilot Development and Opening-up Zone. Intensified economic activity and tourism have accelerated anthropogenic landscape modification, disrupting local ecosystems and increasing landslide susceptibility.

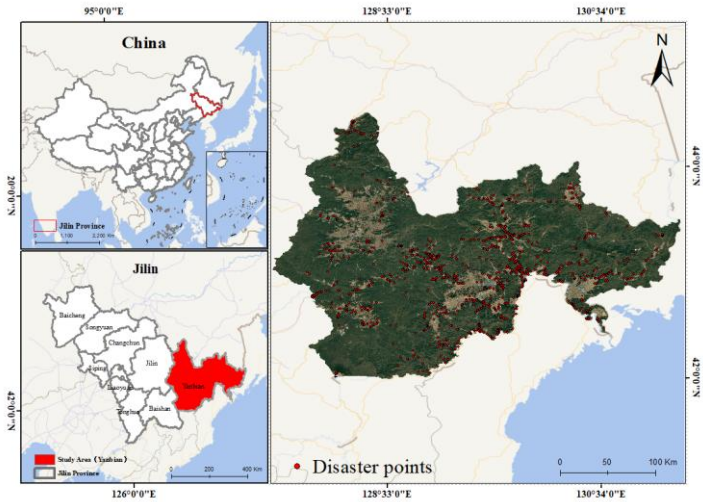

Figure 1: Location map and landslide inventory of Yanbian Prefecture

2.2 Data Sources

The main data sources employed in this study include: (1) 30 m-resolution Copernicus DEM used to extract various topographic, geomorphological, and hydrological factors; (2) 10 m-resolution Sentinel-2A imagery for deriving land cover and NDVI; (3) rainfall records obtained from meteorological stations throughout Yanbian Prefecture; (4) geological maps provided by the Jilin Provincial Geological Bureau; and (5) road network and river data acquired from the Jilin Provincial Department of Transportation and the Jilin Provincial Department of Water Resources, respectively. Table 1 shows the data type and source. These data are used to generate multi-source spatial data that can be used for spatial superposition and model operations after unified in the WGS 1984 projected coordinate system and formatted as unified 30m×30m resolution raster data.

The landslide distribution data for Yanbian Prefecture primarily derive from the Jilin Province Geological Hazard Risk Assessment Survey and the Yanbian Prefecture Monitoring Project, supplemented by data compilation, remote sensing imagery, and field investigations. A total of 313 landslide sites were identified.

Tabel 1: Data and data sources

Data	Sources	Scale
Landslide	Geological disaster risk survey in Jilin Province	
DEM	Copernicus DEM	30m×30m
Remote Sensing Image	Sentinel-2A	10m×10m
Rainfall	Yanbian Prefecture meteorological stations	30m×30m
Geological map	Jilin Provincial Bureau of Geology	1: 500, 000
Road network	Jilin Provincial Transportation Bureau	1: 100, 000
River network	Jilin Provincial Water Resources Bureau	1: 100, 000

2.3 Selection of Landslide Influencing Factors

The selection of influencing factors forms the foundation of susceptibility assessment, as it determines the information that can be incorporated into the modeling process. Because landslide formation is highly complex, there is currently no consensus among scientists on all potential factors. Drawing upon the approach of Huang et al, this study selected factors that are both comprehensive and physically meaningful. Specifically, four categories encompassing eleven indicators were chosen (Figure 2). These four categories include: (1) Topographic factors—elevation, slope, aspect, and curvature; (2) Hydrological factors—annual average rainfall, stream power index (SPI), topographic wetness index (TWI), and distance to rivers; (3) Land cover factors—land use, NDVI, and distance to roads; (4) Lithological factors. Table 2 describes the relationship between various factors and landslide.

Elevation, Slope, Aspect, Curvature, TWI, and SPI were derived and calculated at the same 30m×30m resolution using the Copernicus DEM. Lithology data were obtained from geological maps (1:50,000 scale). For the Distances to roads and rivers, the nearest distance from landslide disaster points to the nearby line objects was computed. Rainfall data collected from meteorological stations were interpolated into raster thematic maps using the inverse distance weighting (IDW) method.

Table 2: Relationship Between Various Factors and Landslide.

Influencing Factors	Description
Elevation	Elevated terrain often receives intense precipitation and snowmelt, increasing soil saturation and promoting landslide initiation, particularly on fractured or weathered slopes.
Slope	Steep slopes are inherently less stable due to enhanced gravitational forces acting on soil and rock masses.
Aspect	Aspect regulates solar radiation exposure, shaping microclimates through variations in soil moisture and temperature.
Curvature	Curvature affects water flow convergence, slope erosion, and soil stability.
Landuse	Land use directly affects vegetation protection, hydrological processes, and surface stability.
TWI	An indicator of surface water accumulation potential.
Lithology	Influencing the supply of slope materials, mechanical stability, and hydrological processes.
NDVI	Reflecting vegetation coverage.
Annual average Rainfall	Precipitation erodes surface materials, while rainwater infiltration erodes the slope interior.
Distance to Road	Blasting and excavation during road construction undermine slope base stability.
Distance to River	Areas near rivers are subject to stronger water erosion.

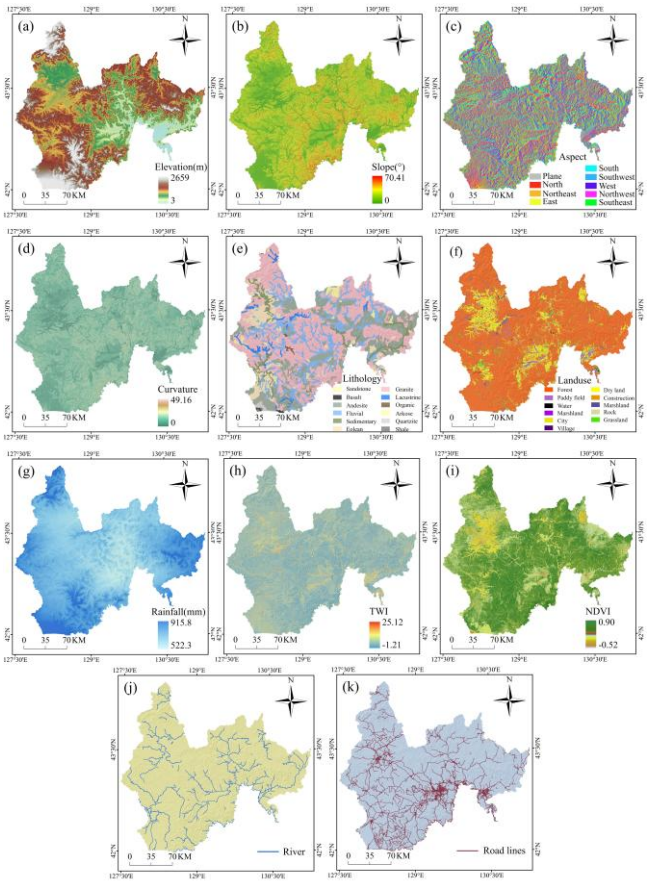

Figure 2: Influencing Factors: (a) Elevation, (b) Slope, (c) Aspect, (d) Curvature, (e) Lithology, (f) Landuse, (g) Rainfall, (h) TWI, (i) NDVI, (j) Distance to Rivers, (k) Distance to Roads

3. Methodology

3.1 Evaluation Unit

In susceptibility studies, commonly used evaluation units include grid units, slope units, and watershed units (Huang et al., 2021a; Lv et al., 2023; Qin et al., 2019). As the

fundamental carriers of all information in the susceptibility evaluation process, selecting appropriate evaluation units is a crucial prerequisite for ensuring the quality of subsequent research. Among these, grid units, usually based on DEM data, divide the study area into regular grids and are the most commonly used units in landslide susceptibility evaluation. However, the regularity of grid units may not effectively reflect certain topographic features, especially in complex mountainous and canyon areas (Alvioli et al., 2016). Slope units, which are geomorphologically homogeneous units based on terrain curvature and watershed boundaries, are more suitable for analyzing the control of local topography (such as slope and curvature) on landslide initiation. However, they may fragment the complete path of landslide from the source area to the flow zone, providing a weaker representation of hydrological connectivity. In contrast, watershed units, as the fundamental units for landslide events, naturally match the entire process of landslide from source to flow to accumulation, making them more suitable for landslide susceptibility evaluation from a hydrological analysis perspective (Qin et al., 2019).

In this study, the ArcGIS Pro hydrological analysis tools were used to extract watershed units based on 30m resolution DEM data for Yanbian Prefecture. First, the DEM data was preprocessed with sink filling, and the ArcSWAT model with a multi-directional flow algorithm and the "burn-in" method was applied to enhance the accuracy of river network extraction. Then, river network nodes were extracted using watershed thresholds of 5 km² and 10 km², respectively, to create sub-watersheds, which were compared with remote sensing images. The results showed that the watershed units extracted using the 5 km² threshold performed better for Yanbian Prefecture. Finally, a total of 35,505 watershed units were extracted in Yanbian Prefecture, among which 313 historical landslide events were located in 297 watershed units as positive samples. An equal number 297 of non-landslide watershed units were randomly selected as negative samples. Following previous work (Tian et al., 2025), the dataset was divided into training and validation sets in a 7:3 ratio.

3.2 Ensemble Learning Algorithm

3.2.1 Bagging

Bagging is an ensemble learning method proposed by Breiman (Breiman 1996), which aims to improve the stability and accuracy of predictions by reducing the variance of the model. For a given training set $D = \{(x_1, y_1), (x_2, y_2), \dots, (x_N, y_N)\}$, The process of the Bagging algorithm can be represented by the following steps:

1) From the original training dataset D, Bootstrap sampling is applied to randomly select N samples, generating K subsets D_k (each subset has a size of N).

2) For each subset D_k, train a base classifier $f_k(x)$

$$f_k(x) = \text{ Model trained on } \mathcal{D}_k \quad (1)$$

3) For a new input sample x, each base classifier makes a prediction $f_k(x)$. The final prediction result is obtained by voting or averaging:

For classification problems (Hard Voting):

$$\hat{y} = \arg\max_y \sum_{k=1}^{K} \mathbb{I}(f_k(x) = y) \quad (2)$$

3.2.2 Stacking

Stacking is a layered ensemble algorithm approach aimed at improving modeling performance by combining different algorithms such as CART, MARS, and Lasso into a learner, as proposed by Wolpert (Kardani et al., 2021; Wolpert 1992). Typically, Stacking involves two levels of learners. In level 0, various ML algorithms are combined to generate a meta-dataset from the original training set. Then, in level 1, the meta-dataset is used to train a meta-learner, which ultimately produces the final result. Figure 3 provides a simple flowchart of the Stacking algorithm. Compared to Bagging, Stacking enhances the predictive power of classifiers. This ensemble method has proven to be highly effective in various fields, including remote sensing, computer science, and finance.

The Stacking method integrates multiple base learners through a meta-learner, making the choice of the meta-learner crucial. Generally, to prevent overfitting, the structure of the meta-learner should be as simple as possible. In this study, logistic regression (LR) (Su et al., 2012) is used as the meta-learner.

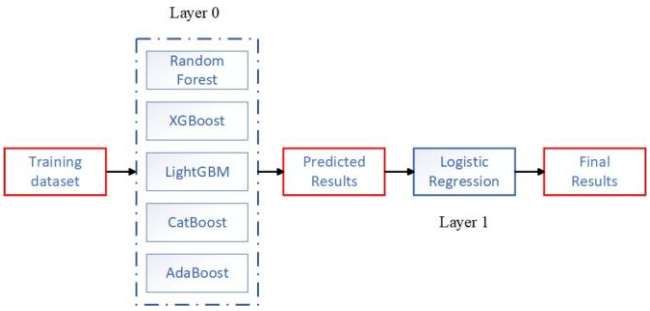

Figure 3: Flowchart of the Stacking algorithm

3.2.3 Voting

The characteristic of the voting algorithm is its simple structure (Parhami 1994). It determines the final classification result by aggregating the predictions from multiple classifiers through voting. In binary classification problems, Soft Voting is typically used. Assume we have N base classifiers, and each classifier outputs a predicted probability for each class. For each sample x, assume there are C classes (labels).

For each base classifier i, the predicted probability for class cc is $P(c \mid x)^{(i)}$. Assuming we use the average probability, the final predicted probability for class c is:

$$P(c \mid x) = \frac{1}{N}\sum_{i=1}^{N} P(c \mid x)^{(i)} \quad (3)$$

where $P(c \mid x)^{(i)}$ represents the predicted probability from classifier i that sample x belongs to class c. $P(c \mid x)$ represents the average predicted probability for class c across all base classifiers.

The final class prediction $\hat{y}$ will be the class with the highest probability:

$$\hat{y} = \arg\max_c P(c \mid x) \quad (4)$$

3.3 Implementation Details

Base Model Selection. The following principles should be followed when generating a multi-algorithm ensemble model (Sagi and Rokach 2018): First, in order for the ensemble method to leverage the advantages of various algorithms, the base learners should be as diverse as possible; Secondly, in order to not affect the accuracy of the final model, the algorithms need to have high predictive performance. Based on the above principles, this paper selects five ML algorithms (Including Random Forest, XGBoost, LightGBM, CatBoost, and AdaBoost.). Their structures and learning approaches differ, with some focusing on the rules for node splitting (decision tree series), while others emphasize weighted combination and boosting (boosting series). This diversity helps minimize errors caused by algorithm instability.

Numerical processing during sampling. During the training process of base models, different features often have different scales. If the data is not preprocessed, some models may fail to exhibit their true predictive performance. Therefore, we apply normalization to the data before model training. The normalization formula is as follows:

$$X_{\text{norm}} = \frac{X - X_{min}}{X_{max} - X_{min}} \quad (5)$$

Where X is the original data, X_{min} is the minimum value in the data, X_{max} is the maximum value in the data, X_{norm} is the normalized data.

Model related settings. In a multi-algorithm ensemble, selecting the appropriate combination of base learners is a challenging task. As the number of base learners increases, the number of possible combinations grows exponentially, making it impractical to manually search for these combinations. For the combination of base learners, there are generally two strategies: one is algorithms like (ABC) (Karaboga 2010), which aim to exchange space for time by consuming more resources to reduce time. However, this algorithm is prone to getting stuck in local optima, meaning it does not necessarily find the optimal combination. The other strategy is to exchange time for space, which aims to consume more time in order to achieve better results. In this study, due to the use of a small sample dataset for rapid training, a grid search method is employed to determine the optimal combination of base learners. In this process, the multi-algorithm ensemble serves as the model to be optimized, and the base learners are treated as discrete parameters. The grid is divided with a step size of 1, and all parameters are traversed.

Model Accuracy. To perform a performance comparison, we considered statistical metrics such as Accuracy, Precision, Cohen's kappa, and F1-score (Yao et al., 2022), as shown in Formula 6.

$$\begin{aligned} \text{Accuracy} &= \frac{TP+TN}{TP+FP+TN+FN}, \\ FI-\ \text{score} &= \frac{2TP}{2TP+FP+FN}, \\ kappa &= \frac{P_o - P_e}{1-P_e} \end{aligned} \quad (6)$$

Where TP, TN, FP and FN represent true positive, true negative, false positive, and false negative, respectively; P_o is the observed agreement proportion; P_e is the expected agreement proportion. Additionally, we also calculated the AUC (Area Under the Receiver Operating Characteristic Curve).

3.4 SHAP

Traditional models (such as linear regression, decision trees, etc.) are relatively simple and easy to interpret. However, with the development of machine learning technology, more and more complex models have started to replace these traditional methods (Zhang et al., 2023). In particularly, deep learning and ensemble learning methods make decisions through multiple layers and nonlinear relationships, which allow them to achieve better performance on many tasks than traditional models. However, this complexity has significantly reduced the interpretability of the models, making it difficult for data scientists to understand how these models reason and make predictions. The design goal of SHAP is to address the above-mentioned issues (Lundberg 2017). It introduces Shapley values, a concept from game theory used to fairly allocate the rewards in a cooperative game. SHAP uses Shapley values to assign an exact contribution value to each feature, which represents the impact of that feature on the final prediction result.

The Shapley value is typically calculated based on Formula 7, which computes the importance of a feature by calculating its marginal contribution across all possible permutations of features.

$$\phi_i(f) = \sum_{S \subseteq N \setminus \{i\}} \frac{|S|!(|N|-|S|-1)!}{|N|!} [f(S \cup \{i\}) - f(S)] \quad (7)$$

Where $\phi_i(f)$ is the Shapley value for feature i, representing the contribution of feature i to the prediction. N is the set of all features. S is a subset of features from N excluding i. $f(S)$ is the model's prediction using the subset of features S.

4. Results

4.1 Model Performance and Evaluation

The landslide inventory and its associated influencing factors were partitioned into training and testing sets and subsequently imported into the Python environment. The model construction process is illustrated in Figure 4 To reduce uncertainties during the training and testing phases, this study employed the Particle Swarm Optimization (PSO) method to provide hyperparameters for the base classifier. PSO is a swarm intelligence–based optimization algorithm that simulates the collective behavior of social animals (flocks of birds, schools of fish e.g.), leveraging information sharing among individuals in the population to seek an optimal solution. By setting the gradient descent objective function to 1−AUC, the loss function was continuously minimized until convergence. As the number of iterations increased, the loss value gradually declined and ultimately reached its minimum, indicating a satisfactory training process.

Subsequently, we used the area under the ROC curve (AUC) as the primary metric to evaluate predictive and generalization capabilities. In addition, Cohen's Kappa (Kappa) and overall accuracy (ACC) were employed as supplementary quality indicators to further assess overall performance (Table 5). In

general, AUC values are interpreted as follows: excellent (0.9–1.0), very good (0.8–0.9), good (0.7–0.8), fair (0.6–0.7), and poor (0.5–0.6). The Kappa coefficient indicates the strength of agreement in the following ranges: almost perfect (0.8–1.0), substantial (0.6–0.8), moderate (0.4–0.6), fair (0.2–0.4), slight (0–0.2), and poor (≤0). ACC, expressed in decimal form, represents the proportion of landslide occurrences and non-occurrences that are correctly classified, with values ranging from 0 to 1. The final hyperparameter configurations and performance metrics are presented in Table 4.

Figure 4 illustrates the overall performance of the base and ensemble models for landslide susceptibility, as measured by the area under the ROC curve (AUC). The results indicate that the Stacking model achieves the highest AUC value (0.957), followed by the Bagging model (0.936). Among the base models, the overall performance is ranked as follows: CatBoost > XGBoost > Random Forest > LightGBM > AdaBoost. Considering these AUC values, it is evident that all models achieved favorable results, with the stacking model based on these tree-based models emerging as the most influential ensemble approach by enhancing the predictive performance of the homogeneous models.

Table 4: The parameter sets used for each model, along with performance metrics (AUC – area under the ROC curve, ACC – Accuracy, and Kappa – Cohen's kappa).

Model	Hyper-parameters	AUC	ACC	Kappa	F1
RF	n_estimators=160 min_samples_split=7 min_samples_leaf=4 max_depth=13	0.909	0.82	0.79	0.85
Xgboost	colsample_bytree=0.8 max_depth=3 n_estimators=100 subsample=0.9	0.91	0.86	0.72	0.88
LightGBM	subsample=0.8 n_estimators=100 max_depth=10 num_leaves=31	0.892	0.81	0.63	0.86
AdaBoost	base_estimator=DT base_estimator__max_depth=4 n_estimators=100	0.872	0.84	0.67	0.8
CatBoost	learning_rate=0.05 iterations=300 depth=8	0.923	0.88	0.77	0.89
Stacking	/	0.957	0.85	0.78	0.86
Bagging	base_estimator=DT base_estimator__max_depth=4 n_estimators=100	0.936	0.87	0.74	0.85
Voting	/	0.901	0.81	0.62	0.86

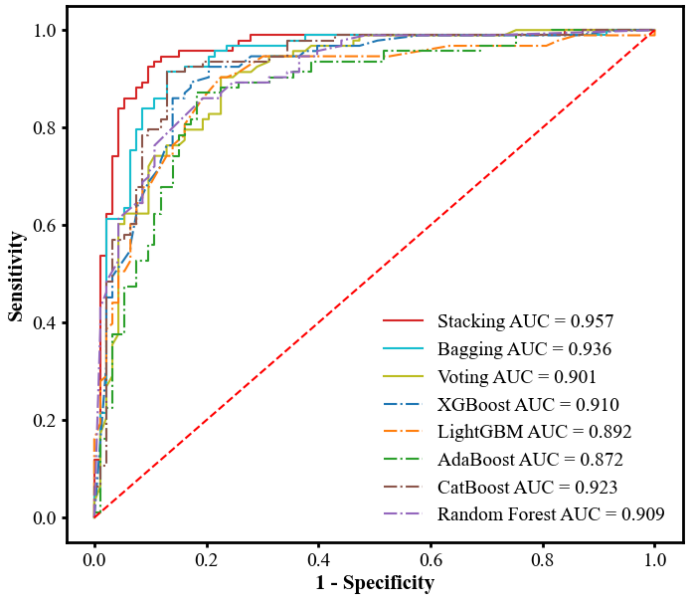

Figure 4: AUC results of the models using validating dataset

4.2 Landslide Susceptibility Maps

To further analyze the predictive performance of the ensemble algorithms, the trained models (Stacking, Bagging, and Voting) were applied to the study area. Each watershed unit was assigned a landslide occurrence probability, which was then imported into a GIS environment. The natural breaks method classified susceptibility into five categories: very low, low, medium, high, and very high. The susceptibility zoning map and corresponding area percentages are presented in Figure 5 As shown in the figure, the generated susceptibility zones successfully identified areas corresponding to early landslide events (the very high and high susceptibility zones), and the spatial distributions of the results from the three models were similar, indicating that all three models effectively reflect the development characteristics and spatial

trends of geological hazards in the study area.

Based on the area percentages of the three ensemble models, landslide susceptibility in the study area exhibits distinct spatial distribution differences. Very low and low susceptibility zones account for approximately 66% of the total area, with the very low susceptibility zones being the most widely distributed and generally forming contiguous patches. In contrast, the high and very high susceptibility zones are concentrated in the central and western parts, forming linear clusters and accounting for about 22% of the total area. This region is critical for landslide hazard prevention and management, warranting enhanced monitoring.

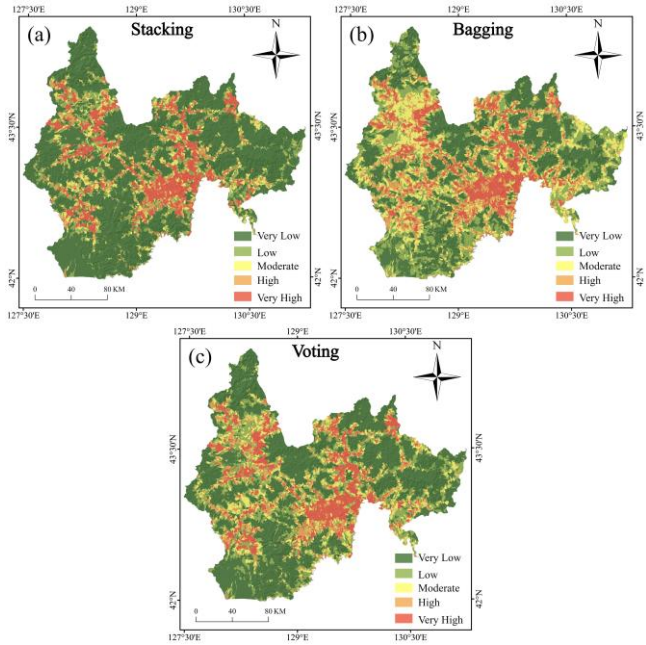

Figure 5: Landslide susceptibility maps: (a) Stacking, (b) Bagging, (c) Voting

5. Discussion

5.1 SHAP Model Interpretation

Landslides have complex causes, and identifying the primary influencing factors can provide valuable guidance for landslide disaster management. In this study, we adopt the Shapley Additive Explanations (SHAP) algorithm to quantitatively evaluate how each factor contributes to the model's predictions. The main calculation procedure is as follows: by considering all possible combinations of influencing factors in the samples, we compute the probability of landslide occurrence with and without each factor. The larger the absolute value of the resulting Shapley value, the more important the factor. Figure 6 presents the ranking of influencing factors in the study area and the SHAP summary plot. In the blue bar chart, the factors are ordered based on the absolute mean Shapley values. It can be observed that distance to roads, rainfall, and NDVI exert the greatest influence on landslide occurrence in this region. Consequently, in geological hazard risk assessment and management, these factors should receive heightened attention, and targeted prevention and mitigation measures should be implemented. In contrast, factors such as TWI, lithology, and aspect show no significant impact on landslide occurrence here. The violin plot shows that samples with lower distance values (blue group) are mostly located to the right of the zero line. This suggests that closer proximity to roads is associated with higher predicted landslide susceptibility. To visually illustrate how variations in the values of key factors affect landslide susceptibility, single-factor dependence plots for the top three factors are provided. This approach enhances the model's transparency and interpretability (Figure 7).

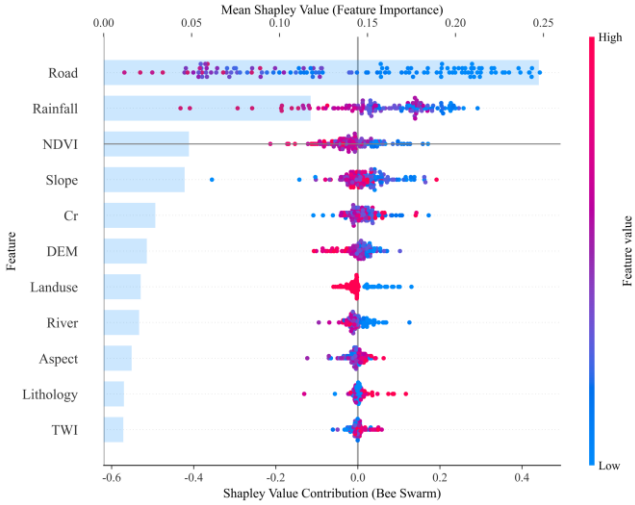

Figure 6: Feature permutation for overall Yanbian.

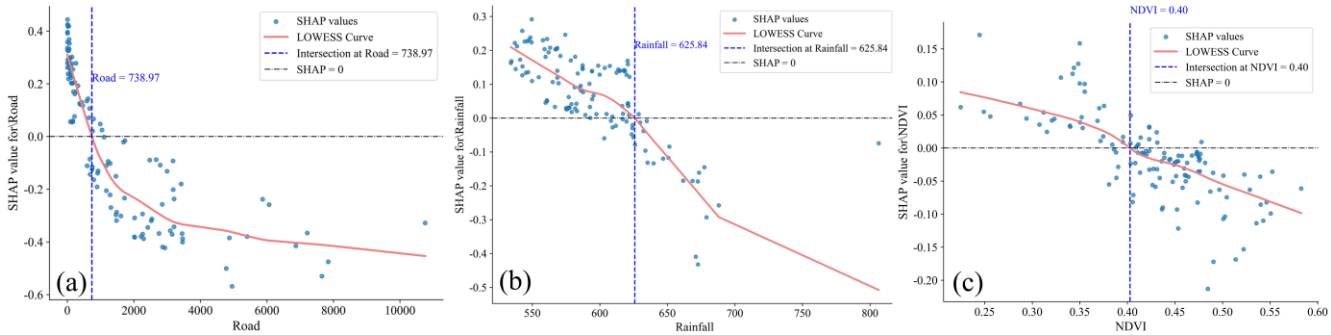

Figure 7: SHAP Dependence Plots: (a) Road, (b) Rainfall, (c) NDVI

When the distance to roads is less than 738 m, it promotes landslide occurrence, and the closer the distance, the stronger the promoting effect becomes (Figure 7a). In the study area, most of the extremely high and high landslide susceptibility zones are located near roads. On the one hand, road construction often entails the removal of large swathes of vegetation and topsoil, potentially leading to exposed spoil heaps or waste disposal sites. If protective measures are inadequate, these areas are prone to sediment scouring during periods of heavy rainfall or snowmelt. Once the eroded

materials enter slopes or gullies, they can evolve into landslide initiation sources. On the other hand, the apparent high importance of "distance to roads" may be partially attributed to limitations in hazard investigations. Although we supplemented the historical landslide data with remote sensing imagery, potential biases in field surveys cannot be entirely eliminated. Overall, the closer a site is to roads, the more pronounced the impacts of construction, drainage, and vegetation destruction become, leading to a generally higher risk of landslides and related geological hazards. Therefore, in engineering practice, it is necessary to plan and design roads scientifically to minimize disturbances to the geological environment caused by road construction. Simultaneously, strengthening monitoring and protective measures for key road-adjacent areas, especially those with steep slopes and concentrated drainage, is essential for effectively reducing both the likelihood of landslide occurrences and the associated losses.

When the multi-year average rainfall is below 625 mm, it strongly promotes landslide occurrence, after which this promoting effect weakens (Figure 7b). The occurrence of landslides depends on the gradual accumulation of loose materials within a specific area, reaching a certain thickness and scale. When rainfall is moderate, it both facilitates rock weathering and soil fragmentation—generating loose materials—and provides a relatively stable environment that allows these materials to accumulate in gullies or at the foot of slopes, forming potential landslide source areas. Under such conditions, once locally accumulated materials encounter a triggering event (short-term heavy rainfall e.g.), they are likely to become unstable and induce landslides. However, when rainfall is excessive, the situation changes dramatically. Prolonged, intense rainfall continuously scours the slopes, carrying away or dispersing loose materials over a wider area before they have a chance to sufficiently accumulate; as a result, forming a concentrated source locally becomes difficult. This continual scouring not only disrupts the material-accumulation process but also "dilutes" or even directly removes potential source materials that might otherwise build up. Consequently, while increases in rainfall up to a certain point can facilitate the formation of loose material, excessive rainfall instead impedes its incremental accumulation and thus inhibits landslide occurrence (Anderson and Sitar 1995; Crosta and Frattini 2008).

Figure 7c illustrates the intrinsic relationship between vegetation coverage and landslide occurrence. As an important indicator of surface vegetation quality, NDVI is significantly negatively correlated with landslide risk. In areas with low NDVI values (< 0.4), vegetation degradation reduces both soil water retention capacity and shear strength, making these regions more susceptible to landslides under heavy rainfall and human engineering activities. In contrast, areas with high NDVI benefit from enhanced friction angle and cohesion provided by plant root systems, thereby forming an effective soil and water conservation barrier (Zhao et al., 2020).

5.2 Ensemble Learning Applied to Landslide Susceptibility

Accurate and timely mapping of landslide susceptibility can significantly inform the spatial distribution of landslide risk, thereby assisting government policy-making and enhancing disaster management capabilities. A comprehensive analysis of the susceptibility zoning map and landslide survey results in the study area reveals consistency between the two; however, the results obtained from different methods exhibit some differences. We found that ensemble learning models generally outperform individual machine learning models due to their significant advantages in reducing variance and bias, as well as enhancing model robustness and generalization capability (Dietterich 2002; Dong et al., 2020). Nevertheless, our validation results indicate that ensemble learning does not always guarantee favorable outcomes. In many susceptibility studies, the distinct characteristics of various machine learning models mean that different models may be applicable to different regions, with multiple models often being suitable for the study area. Ensemble learning, as a framework strategy, can transform weaker classifiers into robust models tailored to specific problems. Specifically, Stacking exploits the predictive features of different models and automatically learns optimal fusion weights via a meta-learner (Pavlyshenko 2018); Bagging focuses on reducing variance through random sampling and voting/averaging of results (Quinlan 1996); and Voting is the simplest and most easily implemented post-fusion method (Parhami 1994).

Yanbian Prefecture lies within a geologically active and topographically rugged mountainous region, where landslides occur frequently and pose serious threats to both human safety and ecological stability. In this context, developing science-based disaster prevention strategies is an urgent priority. By enabling both predictive accuracy and interpretable insights into physical drivers, this study offers a robust framework for region-specific risk management.

Based on the findings, we propose the following recommendations:

(1) Targeted risk zoning — High-susceptibility areas should be delineated based on susceptibility mapping and dominant triggering factors. Differentiated land-use planning that balances ecological protection with infrastructure development can reduce disaster risks associated with human disturbances.

(2) Enhanced community resilience — In areas of high and very high susceptibility, emergency shelter networks should be expanded, regular preparedness training established, and public awareness strengthened through education campaigns and drills to improve self- and mutual-aid capabilities.

(3) Intelligent early warning systems — A dynamic, high-resolution monitoring framework should be developed by integrating UAV-based inspections, real-time remote sensing, big data analytics, and machine learning. This would enhance both the spatial accuracy and timeliness of landslide forecasting.

5.3 Limitations and Outlook

While the ensemble models demonstrated strong predictive skill and interpretability, several limitations remain. The landslide inventory, although enhanced with remote sensing,

may underrepresent events in inaccessible terrain or underreported periods. Key dynamic triggers—such as near-real-time rainfall intensity, antecedent soil moisture, and anthropogenic disturbances—were unavailable and thus excluded, potentially limiting the temporal responsiveness of the model. Moreover, SHAP-based interpretation, while insightful, adds computational overhead as model complexity scales.

Future work should integrate high-temporal-resolution meteorological and hydrological data to capture transient triggering conditions. Hybrid approaches combining data-driven models with physically based process simulations may improve early warning accuracy. Finally, testing the framework across varied topographies and tectonic settings will be crucial to assess its robustness and transferability for broader hazard mitigation strategies.

6. Conclusion

This study combines ensemble learning with the SHAP method, which not only enhances the accuracy of landslide susceptibility prediction but also interprets the results of the Stacking model by analyzing both global and local interdependencies. The main conclusions are as follows:

(1) To address the uncertainty inherent in a single model, this study employs multiple base models and integrates them using methods such as Stacking, Bagging, and Voting. Among these, Stacking demonstrated the best performance due to its higher prediction accuracy.

(2) The SHAP algorithm was employed to interpret the Stacking model, revealing the contributions of various influencing factors to landslide prediction. The results indicate that road proximity, rainfall, and NDVI are the primary factors affecting landslide hazards in Yanbian Prefecture.

(3) Landslide hazards in Yanbian Prefecture generally exhibit a spatial pattern of being higher in the west and lower in the east, with distinct band-like and spatial clustering characteristics. Extremely high and high susceptibility areas are mainly concentrated in the western and central regions, whereas low susceptibility areas are primarily distributed in the eastern region.

CRediT Authorship Contribution Statement

Shuhao Dong: Conceptualization, Methodology, Formal analysis, Investigation, Writing – original draft. Shengwu Qin: Project administration, Funding acquisition., Validation, Formal analysis, Resources, Data curation, Writing – review & editing. Jiangfeng Lv: Validation, Investi gation, Supervision, Project administration. Jiasheng Cao: Investigation, Supervision. Jingyu Yao: Software, Data curation. Zhenmin Chen: Conceptualization, Supervision.

Funding

This study was supported by the Natural Science Foundation of China [Grant numbers 41977221 and 41972267].

Acknowledgments

The authors are also thankful to the anonymous reviewers for their valuable feedback on the manuscript.

References

[1] Alvioli, M., Marchesini, I., Reichenbach, P., Rossi, M., Ardizzone, F., Fiorucci, F., Guzzetti, F. 2016. Automatic delineation of geomorphological slope units with r. slopeunits v1. 0 and their optimization for landslide susceptibility modeling[J]. Geoscientific Model Development. 9, 3975-3991. https://doi.org/10.5194/gmd-9-3975-2016

[2] Anbalagan, R., Singh, B. 1996. Landslide hazard and risk assessment mapping of mountainous terrains—a case study from Kumaun Himalaya, India[J]. Engineering Geology. 43, 237-246. https://doi.org/10.1016/S0013-7952 (96)00033-6

[3] Anderson, S.A., Sitar, N. 1995. Analysis of rainfall-induced landslides[J]. Journal of Geotechnical Engineering. 121, 544-552. https://doi.org/10.1061/(ASCE)0733-9410 (1995)121:7 (544)

[4] Breiman, L. 1996. Bagging predictors[J]. Machine learning. 24, 123-140. https://doi.org/10.1007/BF00058655

[5] Chen, W., Pourghasemi, H.R., Naghibi, S.A. 2018. Prioritization of landslide conditioning factors and its spatial modeling in Shangnan County, China using GIS-based data mining algorithms[J]. Bulletin of Engineering Geology and the Environment. 77, 611-629. https://doi.org/10.1007/s10064-017-1004-9

[6] Chen, W., Shirzadi, A., Shahabi, H., Ahmad, B.B., Zhang, S., Hong, H., Zhang, N. 2017a. A novel hybrid artificial intelligence approach based on the rotation forest ensemble and naïve Bayes tree classifiers for a landslide susceptibility assessment in Langao County, China[J]. Geomatics, Natural Hazards and Risk. 8, 1955-1977. https://doi.org/10.1080/19475705.2017.1401560

[7] Chen, W., Xie, X., Wang, J., Pradhan, B., Hong, H., Bui, D.T., Duan, Z., Ma, J. 2017b. A comparative study of logistic model tree, random forest, and classification and regression tree models for spatial prediction of landslide susceptibility[J]. Catena. 151, 147-160. https://doi.org/10.1016/j.catena.2016.11.032

[8] Constantin, M., Bednarik, M., Jurchescu, M.C., Vlaicu, M. 2011. Landslide susceptibility assessment using the bivariate statistical analysis and the index of entropy in the Sibiciu Basin (Romania)[J]. Environmental earth sciences. 63, 397-406. https://doi.org/10.1007/s12665-010-0724-y

[9] Corominas, J., van Westen, C., Frattini, P., Cascini, L., Malet, J.-P., Fotopoulou, S., Catani, F., Van Den Eeckhaut, M., Mavrouli, O., Agliardi, F. 2014. Recommendations for the quantitative analysis of landslide risk[J]. Bulletin of Engineering Geology and the Environment. 73, 209-263. https://doi.org/10.1007/s10064-013-0538-8

[10] Crosta, G.B., Frattini, P. 2008. Rainfall-induced landslides and landslides[J]. Hydrological Processes: An International Journal. 22, 473-477. https://doi.org/10.1002/hyp.6885

[11] Cui, P., Zou, Q., Xiang, L.-z., Zeng, C. 2013. Risk assessment of simultaneous landslides in mountain townships[J]. Progress in Physical geography. 37, 516-542. https://doi.org/10.1177/0309133313491445
[12] Di Napoli, M., Carotenuto, F., Cevasco, A., Confuorto, P., Di Martire, D., Firpo, M., Pepe, G., Raso, E., Calcaterra, D. 2020. Machine learning ensemble modelling as a tool to improve landslide susceptibility mapping reliability[J]. Landslides. 17, 1897-1914. https://doi.org/10.1007/s10346-020-01392-9
[13] Dietterich, T.G. 2002. Ensemble learning[J]. The handbook of brain theory and neural networks. 2, 110-125.
[14] Dikshit, A., Pradhan, B., Alamri, A.M. 2021. Pathways and challenges of the application of artificial intelligence to geohazards modelling[J]. Gondwana Research. 100, 290-301. https://doi.org/10.1016/j.gr.2020.08.007
[15] Dong, X., Yu, Z., Cao, W., Shi, Y., Ma, Q. 2020. A survey on ensemble learning[J]. Frontiers of Computer Science. 14, 241-258. https://doi.org/10.1007/s11704-019-8208-z
[16] Dou, J., Yunus, A.P., Bui, D.T., Merghadi, A., Sahana, M., Zhu, Z., Chen, C.-W., Han, Z., Pham, B.T. 2020. Improved landslide assessment using support vector machine with bagging, boosting, and stacking ensemble machine learning framework in a mountainous watershed, Japan[J]. Landslides. 17, 641-658. https://doi.org/10.1007/s10346-019-01286-5
[17] Ermini, L., Catani, F., Casagli, N. 2005. Artificial neural networks applied to landslide susceptibility assessment[J]. Geomorphology. 66, 327-343. https://doi.org/10.1016/j.geomorph.2004.09.025
[18] Felicísimo, Á.M., Cuartero, A., Remondo, J., Quirós, E. 2013. Mapping landslide susceptibility with logistic regression, multiple adaptive regression splines, classification and regression trees, and maximum entropy methods: a comparative study[J]. Landslides. 10, 175-189. https://doi.org/10.1007/s10346-012-0320-1
[19] Guzzetti, F. 2003. Landslide cartography, hazard assessment and risk evaluation: overview, limits and prospective. Mitigation of Climate Induced Natural Hazard Workshop 3. Proceedings, Wallingford, UK.
[20] Han, Z., Li, Y., Huang, J., Chen, G., Xu, L., Tang, C., Zhang, H., Shang, Y. 2017. Numerical simulation for run-out extent of landslides using an improved cellular automaton model[J]. Bulletin of Engineering Geology and the Environment. 76, 961-974. https://doi.org/10.1007/s10064-016-0902-6
[21] He, J., Zhang, L., Fan, R., Zhou, S., Luo, H., Peng, D. 2022. Evaluating effectiveness of mitigation measures for large landslides in Wenchuan, China[J]. Landslides. 19, 913-928. https://doi.org/10.1007/s10346-021-01809-z
[22] Huang, F., Tao, S., Chang, Z., Huang, J., Fan, X., Jiang, S.-H., Li, W. 2021a. Efficient and automatic extraction of slope units based on multi-scale segmentation method for landslide assessments[J]. Landslides. 18, 3715-3731. https://doi.org/10.1007/s10346-021-01756-9
[23] Huang, F., Ye, Z., Jiang, S.-H., Huang, J., Chang, Z., Chen, J. 2021b. Uncertainty study of landslide susceptibility prediction considering the different attribute interval numbers of environmental factors and different data-based models[J]. Catena. 202, 105250. https://doi.org/10.1016/j.catena.2021.105250
[24] Hutter, K., Svendsen, B., Rickenmann, D. 1994. Landslide modeling: A review[J]. Continuum mechanics and thermodynamics. 8, 1-35. https://doi.org/10.1007/BF01175749
[25] Iversion, R. 1997. The Physics of Landslide. Reviews of Geophysics[J]. https://doi.org/10.1029/97RG00426
[26] Jakob, M., McDougall, S., Weatherly, H., Ripley, N. 2013. Debris-flow simulations on cheekye river, british columbia[J]. Landslides. 10, 685-699. https://doi.org/10.1007/s10346-012-0365-1
[27] Karaboga, D. 2010. Artificial bee colony algorithm[J]. scholarpedia. 5, 6915. https://doi.org/10.4249/scholarpedia.6915
[28] Kardani, N., Zhou, A., Nazem, M., Shen, S.-L. 2021. Improved prediction of slope stability using a hybrid stacking ensemble method based on finite element analysis and field data[J]. Journal of Rock Mechanics and Geotechnical Engineering. 13, 188-201. https://doi.org/10.1016/j.jrmge.2020.05.011
[29] Lin, J., Chen, W., Qi, X., Hou, H. 2021. Risk assessment and its influencing factors analysis of geological hazards in typical mountain environment[J]. Journal of cleaner production. 309, 127077. https://doi.org/10.1016/j.jclepro.2021.127077
[30] Liu, X.-l. 2003. Gully-specific landslide hazard assessment in China[J]. Chinese Geographical Science. 13, 112-118. https://doi.org/10.1007/s11769-003-0003-x
[31] Liu, X., Shu, X., Liu, X., Duan, Z., Ran, Z. 2020. Risk assessment of landslide in Ya'an city based on BP neural network. IOP Conference Series: Materials Science and Engineering. IOP Publishing, 012006. https://doi.org/10.1088/1757-899X/794/1/012006
[32] Lundberg, S. 2017. A unified approach to interpreting model predictions[J]. arXiv preprint arXiv:1705.07874.
[33] Lv, J., Qin, S., Chen, J., Qiao, S., Yao, J., Zhao, X., Cao, R., Yin, J. 2023. Application of different watershed units to landslide susceptibility mapping: A case study of Northeast China[J]. Frontiers in Earth Science. 11, 1118160. https://doi.org/10.3389/feart.2023.1118160
[34] Marcílio, W.E., Eler, D.M. 2020. From explanations to feature selection: assessing SHAP values as feature selection mechanism. 2020 33rd SIBGRAPI conference on Graphics, Patterns and Images (SIBGRAPI). Ieee, 340-347. https://doi.org/10.1109/SIBGRAPI51738.2020.00053
[35] Merghadi, A., Abderrahmane, B., Tien Bui, D. 2018. Landslide susceptibility assessment at Mila Basin (Algeria): a comparative assessment of prediction capability of advanced machine learning methods[J]. ISPRS International Journal of Geo-Information. 7, 268. https://doi.org/10.3390/ijgi7070268
[36] Mokhtari, K.E., Higdon, B.P., Başar, A. 2019. Interpreting financial time series with SHAP values. Proceedings of the 29th annual international conference on computer science and software engineering, 166-172.
[37] Parhami, B. 1994. Voting algorithms[J]. IEEE transactions on reliability. 43, 617-629. https://doi.org/10.1109/24.370218
[38] Pavlyshenko, B. 2018. Using stacking approaches for machine learning models. 2018 IEEE second

international conference on data stream mining & processing (DSMP). IEEE, 255-258. https://doi.org/10.1109/DSMP.2018.8478522
[39] Pellegrino, A.M., di Santolo, A.S., Schippa, L. 2015. An integrated procedure to evaluate rheological parameters to model landslides[J]. Engineering Geology. 196, 88-98. https://doi.org/10.1016/j.enggeo.2015.07.002
[40] Pham, B.T., Tien Bui, D., Prakash, I. 2018. Bagging based support vector machines for spatial prediction of landslides[J]. Environmental earth sciences. 77, 1-17. https://doi.org/10.1007/s12665-018-7268-y
[41] Pradhan, B., Dikshit, A., Lee, S., Kim, H. 2023. An explainable AI (XAI) model for landslide susceptibility modeling[J]. Applied Soft Computing. 142, 110324. https://doi.org/10.1016/j.asoc.2023.110324
[42] Qin, S., Lv, J., Cao, C., Ma, Z., Hu, X., Liu, F., Qiao, S., Dou, Q. 2019. Mapping landslide susceptibility based on watershed unit and grid cell unit: a comparison study[J]. Geomatics, Natural Hazards and Risk. https://doi.org/10.1080/19475705.2019.1604572
[43] Quinlan, J.R. 1996. Bagging, boosting, and C4. 5. Aaai/Iaai, vol. 1. Citeseer, 725-730.
[44] Rickenmann, D., Laigle, D., McArdell, B.W., Hübl, J. 2006. Comparison of 2D debris-flow simulation models with field events[J]. Computational Geosciences. 10, 241-264. 10.1007/s10596-005-9021-3. https://doi.org/10.1007/s10596-005-9021-3
[45] Rigatti, S.J. 2017. Random forest[J]. Journal of Insurance Medicine. 47, 31-39. https://doi.org/10.17849/insm-47-01-31-39.1
[46] Sagi, O., Rokach, L. 2018. Ensemble learning: A survey[J]. Wiley interdisciplinary reviews: data mining and knowledge discovery. 8, e1249. https://doi.org/10.1002/widm.1249
[47] Scheild, C., Rickenmann, D. 2011. TopFlowDF-a simple GIS based model to simulate debris-flow runout on the fan[J]. Italian journal of engineering geology and environment, 253-262.
[48] Shaikhina, T., Lowe, D., Daga, S., Briggs, D., Higgins, R., Khovanova, N. 2019. Decision tree and random forest models for outcome prediction in antibody incompatible kidney transplantation[J]. Biomedical Signal Processing and Control. 52, 456-462. https://doi.org/10.1016/j.bspc.2017.01.012
[49] Shen, S., Liao, W., Nie, L., Xu, Y., Zhang, M. 2018. Landslide hazard assessment at Dongmatun Village in Laomao mountainous area of Dalian, Northeast China[J]. Arabian Journal of Geosciences. 11, 1-12. https://doi.org/10.1007/s12517-018-3953-0
[50] Su, X., Yan, X., Tsai, C.L. 2012. Linear regression[J]. Wiley Interdisciplinary Reviews: Computational Statistics. 4, 275-294. https://doi.org/10.1002/wics.1198
[51] Tian, Y., Wu, Z., Cui, S., Hong, W., Wang, B., Li, M. 2025. Assessing Wildfire Susceptibility and Spatial Patterns in Diverse Forest Ecosystems Across China: An Integrated Geospatial Analysis[J]. Journal of cleaner production, 144800. https://doi.org/10.1016/j.jclepro.2025.144800
[52] Tsangaratos, P., Ilia, I. 2016. Comparison of a logistic regression and Naïve Bayes classifier in landslide susceptibility assessments: The influence of models complexity and training dataset size[J]. Catena. 145, 164-179. https://doi.org/10.1016/j.catena.2016.06.004
[53] Tsangaratos, P., Ilia, I., Hong, H., Chen, W., Xu, C. 2017. Applying Information Theory and GIS-based quantitative methods to produce landslide susceptibility maps in Nancheng County, China[J]. Landslides. 14, 1091-1111. https://doi.org/10.1007/s10346-016-0769-4
[54] Wang, H., Liang, Q., Hancock, J.T., Khoshgoftaar, T.M. 2024. Feature selection strategies: a comparative analysis of SHAP-value and importance-based methods[J]. Journal of Big Data. 11, 44. https://doi.org/10.1186/s40537-024-00905-w
[55] Wolpert, D.H. 1992. Stacked generalization[J]. Neural networks. 5, 241-259. https://doi.org/10.1016/S0893-6080 (05)80023-1
[56] Yao, J., Qin, S., Qiao, S., Liu, X., Zhang, L., Chen, J. 2022. Application of a two-step sampling strategy based on deep neural network for landslide susceptibility mapping[J]. Bulletin of Engineering Geology and the Environment. 81, 148. https://doi.org/10.1007/s10064-022-02615-0
[57] Zeng, P., Chen, J., Chang, M., Sun, X., Li, T. 2024. Uncertainty characterization, propagation, and evaluation in landslide run-out hazard assessment[J]. Landslides, 1-16. https://doi.org/10.1007/s10346-024-02423-5
[58] Zhang, J., Ma, X., Zhang, J., Sun, D., Zhou, X., Mi, C., Wen, H. 2023. Insights into geospatial heterogeneity of landslide susceptibility based on the SHAP-XGBoost model [J]. Journal of environmental management. 332, 117357. https://doi.org/10.1016/j.jenvman.2023.117357
[59] Zhang, T., Fu, Q., Wang, H., Liu, F., Wang, H., Han, L. 2022. Bagging-based machine learning algorithms for landslide susceptibility modeling[J]. Natural Hazards. 110, 823-846. https://doi.org/10.1007/s11069-021-04986-1
[60] Zhao, P., Wang, D., He, S., Lan, H., Chen, W., Qi, Y. 2020. Driving forces of NPP change in landslide prone area: A case study of a typical region in SW China[J]. Ecological Indicators. 119, 106811. https://doi.org/10.1016/j.ecolind.2020.106811